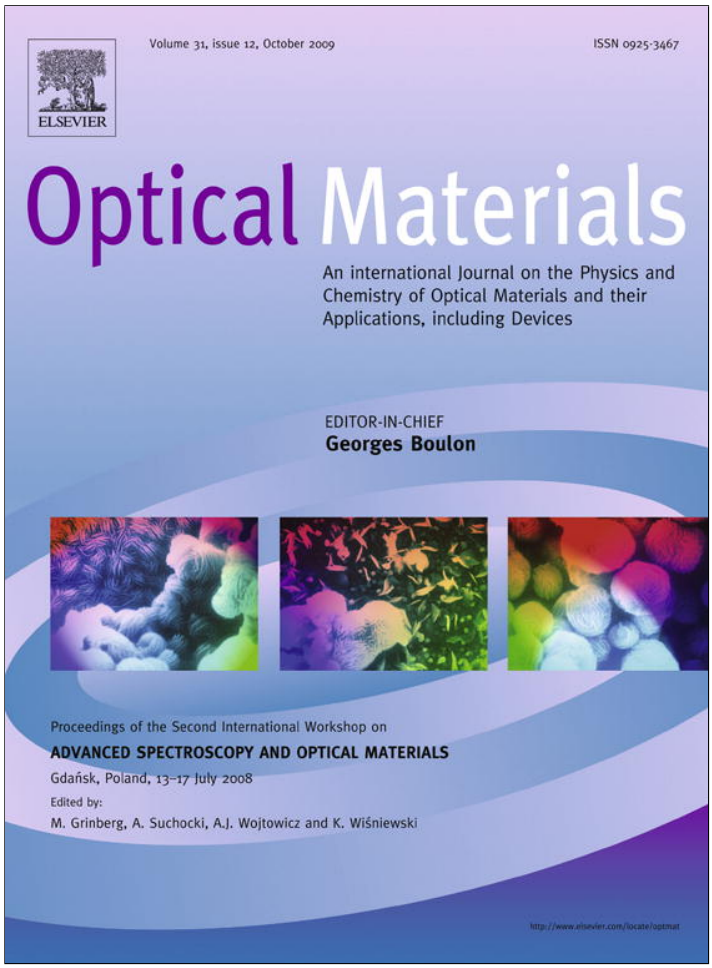

Optical Materials 31 (2009) 1772–1776

Contents lists available at ScienceDirect

Optical Materials

journal homepage: www.elsevier.com/locate/optmat

VUV spectroscopy of wide bandgap materials

Andrzej J. Wojtowicz

Instytut Fizyki, Uniwersytet M. Kopernika, ul. Grudziądzka 5, 87-100 Torun, Poland

ARTICLE INFO

Article history:
Received 8 September 2008
Accepted 10 December 2008
Available online 5 May 2009

PACS:
29.40.Mc
71.20.Ps
71.35.−y
78.55.Hx
78.60.−b

Keywords:
BaF_2:Ce
BaF_2:Er
$(Ba,La)F_2$:Er
UV and VUV spectroscopy
Er^{3+}, Ce^{3+} ions

ABSTRACT

In this paper we will present VUV spectroscopy experiments performed at the Superlumi station of Hasylab, DESY, Hamburg, on samples of BaF_2 crystals activated with Ce and BaF_2, $(Ba,La)F_2$ crystals activated with Er. The results of these experiments include time resolved luminescence and luminescence excitation spectra obtained under wavelength selective VUV and UV excitation by pulsed synchrotron radiation.

We will reveal the information provided by the VUV/UV excitation spectra of the Ce^{3+} $5d \rightarrow 4f$ as well as Er^{3+} $4f^{n-1}5d \rightarrow 4f^n$ and $4f^n \rightarrow 4f^n$ emissions on energy transfer mechanisms from the fluoride host to the rare earth ion. We will demonstrate that the fast energy transfer channels involve bound excitons while the generation of free electrons and holes leads to slower processes dependant on hole and/or electron trapping.

We will demonstrate that differences between the excitation spectra of the $5d \rightarrow 4f$ emission in Ce and $4f^{10}5d \rightarrow 4f^{11}$ emission in Er activated BaF_2 are generated by the coupling of the $4f \rightarrow 5d$ transition to the $4f^{10}$ core of the Er^{3+} ion. We will also identify the additional band, absent for Ce, which is due to the exchange split high spin (HS) state of the $4f^{10}5d$ configuration responsible for the slow decay of the excited Er^{3+} ions in BaF_2 and $(Ba,La)F_2$.

Finally we will provide evidence and explain why the dominant VUV $4f^{10}5d \rightarrow 4f^{11}$ Er^{3+} emission in BaF_2 is spin-forbidden and slow while in the mixed $(Ba,La)F_2$ crystals it is spin-allowed and fast.

1. Introduction

The surge of interest in VUV spectroscopy of solid state materials is largely due to new and demanding applications such as UV and VUV solid state lasers, fast and efficient scintillators and new "quantum-cutting" phosphors driven by mercury-free discharge radiation. At the forefront of materials considered for these attractive new applications are wide bandgap materials activated with rare earth ions.

An important additional incentive is provided by disparity between easily accessible model programs providing energies for a large number of emission and absorption lines of rare earth ions and scarce experimental results especially in the UV and VUV spectral ranges. We note that the so-called "extended Dieke's" diagram based on model calculations partly verified by experiment and covering energies above 40,000 cm^{-1} has been established only recently [1,2]. Experimental verification for some of these energies is still missing [3].

We also note that the VUV excitation spectra of rare earth emissions reflect various mechanisms of energy transfer from the host to the ion enabling evaluation of e.g. scintillator materials. The annual Hasylab reports published on-line provide numerous examples, see e.g.[1].

In this paper we report experimental studies of UV and VUV luminescence from Ce and Er activated crystals of BaF_2 and Er activated mixed crystals of $(Ba,La)F_2$ using wavelength selective, pulsed synchrotron radiation. The results that we have obtained confirm and extend earlier studies of other fluorides [3], as well as provide some new experimental observations, such as fast and efficient VUV emission from $(Ba,La)F_2$:Er.

2. Crystals and experimental set-ups

The Ce and Er doped samples of BaF_2 and $(Ba,La)F_2$ were cut from larger boules grown by Optovac Inc. (North Brookfield, MA, USA) using the Bridgman method. The concentration of Ce in the melt was 0.015 and 0.05 mol% for the Ce-doped boules of BaF_2. The 0.05 mol% boule was co-doped with Na (0.2 mol%) to minimize interstitial fluorine compensation. The Er concentrations in Er-doped boules of BaF_2 were 0.05 and 0.2 mol% in the melt. The $(Ba,La)F_2$ boule contained 30 mol% of La and 0.2 mol% of Er. The samples were not subjected to any chemical reducing procedure. They

E-mail address: andywojt@fizyka.umk.pl

[1] http://www.fizyka.umk.pl/andywojt/physics.htm.

0925-3467/$ - see front matter © 2009 Elsevier B.V. All rights reserved.
doi:10.1016/j.optmat.2008.12.032

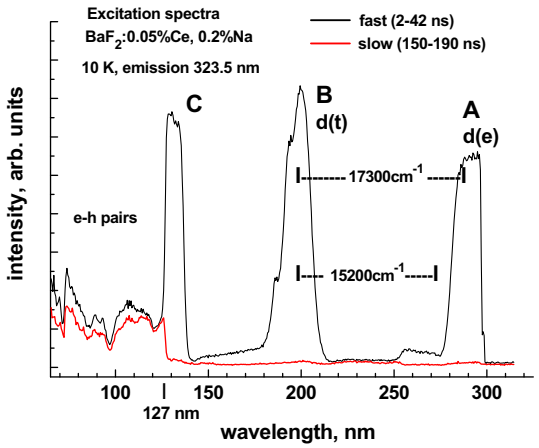

Fig. 1. Time resolved excitation spectra of Ce-emission in BaF_2:0.05 mol%Ce, 0.2 mol%Na at 10 K. The spectra have been corrected using a salicylate standard. Resolution was 0.32 nm, step 0.5 nm. Black line, signal accumulated in the time window set at 2-42 ns ("fast" spectrum), red line, 150–190 ns ("slow" spectrum). For details see text. (For interpretation of the references to colour in this figure legend, the reader is referred to the web version of this article.)

were of high optical quality, clear, displayed no color, no inclusions and no indication of oxygen contamination.

The VUV/UV experiments (luminescence and excitation spectra) were performed at the SUPERLUMI station of HASYLAB on the Doris III storage ring in DESY, Hamburg, Germany. A detailed description of SUPERLUMI's experimental facilities, available online[2], was also given by Zimmerer [4].

For excitation we have used a primary 2 m normal incidence monochromator in 15° McPherson mounting, equipped with the holographic concave grating (1200 groves/mm), coated by Al + MgF_2 (50–330 nm). The resolution was 0.32 nm.

For emission we have used two monochromators: the home-made 0.5 m Pouey VUV monochromator (f/2.8, fixed resolution of 1.1 nm), equipped with the solar blind Hamamatsu R6836 photomultiplier (115–300 nm) for VUV, and the Acton Research 0.3 m Czerny-Turner monochromator "Spectra Pro 300i" (f/4) equipped with the Hamamatsu R6358P photomultiplier for longer wavelengths spectra (200–800 nm). Resolution of this monochromator depended on the adjustable slit width and the grating inserted. We have used three gratings, one having 1200 g/mm (2.7 nm/mm) and blazed at 300 nm and two others having 300 g/mm (10.8 nm/mm) and blazed at 300 and 500 nm, respectively.

3. Experimental results and discussion

In Fig. 1 we present time resolved excitation spectra of the Ce emission (323.5 nm) measured at 10 K from the sample of BaF_2: activated with Ce and Na (0.05 mol%Ce, 0.2 mol%Na). The spectra have been corrected for spectral sensitivity of the set-up using the salicylate standard. The time window used to integrate emission photon counts was set at 40 ns and delay was set at 2 ns for the "fast" spectrum (black solid line) and 150 ns for the "slow" spectrum (red solid line). The "fast" spectrum shows three main bands, labeled A, B and C. The peak position of the A-band (5d(e)) at 291 nm as well as peak position and the structure of the B-band (5d(t)) at about 200 nm are no different that in the corresponding spectrum of the lower Ce concentration (0.015 mol%Ce) sample (not shown) and numerous spectra measured earlier (compare e.g. [5]). We note that positions of the spectrally resolved subbands of the B-band at about 186.5, 194.0 and 199.9 nm, suggest that 10 Dq, at about 17,300 cm^{-1}, is much larger than energies associated with the lower symmetry crystal field component.

Somewhat lower value of 10 Dq (at 15,200 cm^{-1}) is obtained if one assumes that the weak broad band at about 265 nm is due to the forbidden transition to the 5d(e) sublevel split off by the combined action of spin-orbit interaction and lower symmetry crystal field component [6]. We note in passing that 17,300 cm^{-1} value is close to the value of 17,400 cm^{-1} obtained for Ce in CaF_2 by Manthey, who analyzed positions of all d-bands to fully characterize the crystal field [6].

In any case it seems reasonable to assume that in both Na-co-doped and Na-free crystals we are dealing with roughly the same dominant "effective" Ce site of predominantly cubic character. This is not unexpected since the differences in positions of the zero-phonon lines of Ce in various sites in Na-co-doped and Na-free crystals of CaF_2, studied by Hollingsworth and McClure [7], were not large (usually much less than 100 cm^{-1}).

Both d-bands are missing in the "slow" spectrum measured with larger delay (150 ns). This is to be expected since the Ce-emission that follows direct excitation into one of the d-bands decays with the radiative lifetime of about 30 ns [5]. More unusual is the third band, C, positioned between 127 and 140 nm, below the bandgap and the first exciton peak in BaF_2 at 10 K (117 nm and 124 nm respectively, [8]), which also generates fast Ce-emission but is unlikely to be due to any direct transition at Ce^{3+} ion. The seemingly obvious interpretation involving free excitons is unlikely since the first excitonic peak corresponds to the reflection peak and, consequently, a dip in the excitation spectrum at about 120 nm. We also note that excitation into the first excitonic peak favors a well known excitonic emission (self-trapped exciton, STE, see e.g. [5]). These observations explain a steep decrease of the C-band at the short wavelength side and emphasize the need to invoke a different interpretation of the C-band itself.

We propose that the C-band is due to an unrelaxed state of the exciton bound to Ce^{3+} ion. The energy transfer to one of 5d states of the Ce^{3+} ion, facilitated by some preceding lattice relaxation, is likely to be very efficient and fast, as observed in the experiment.

In addition to the 121.4 nm dip we note also three other dips; at 96.8, 85.2 and 72.8 nm. These dips correspond to other reflection peaks reported earlier [8].

A good VUV sensitivity is expected and desired for scintillation detector material. Although, in BaF_2:Ce the emission is due almost exclusively to Ce ions and not to STEs and VUV response is good but, unfortunately, it is characterized by long decay times [5]. Despite a significant fast component, a large fraction of energy transferred to Ce-ions by this channel (most likely via free electron-hole pairs) is intercepted by traps responsible for slow components in the scintillation time profile of BaF_2:Ce.

The earlier Superlumi measurements of emission and excitation spectra of Er^{3+} in BaF_2 have already been reported for the 0.2 mol% Er sample [9]. Since there was no difference between "fast" and "slow" time window spectra, in Fig. 2 we show some of the recently measured time-integrated excitation spectra of the Er^{3+} VUV and VIS emissions from a different BaF_2 sample doped with 0.05 mol% Er.

The red and blue lines show the spectrum measured at two wavelengths (163.5 and 165 nm, res. 1.1 nm, step 0.1 and 0.01 nm, respectively) of the VUV emission band peaking at 163.5 nm. The black line shows the spectrum measured at 547 nm corresponding to the well known "green" emission from Er ($^4S_{3/2}$ to $^4I_{15/2}$). While d-bands, dominating the 163.5 and 165 nm spectra, are missing, there is a strong band in the 547 nm spectrum, centered at about 131 nm that clearly resembles the C-band in the excitation spectrum of Ce emission. It seems reasonable, therefore, to assume that this band is due to the Er-bound

[2] http://hasylab.desy.de/facilities/doris_iii/beamlines/i_superlumi/index_eng.html.

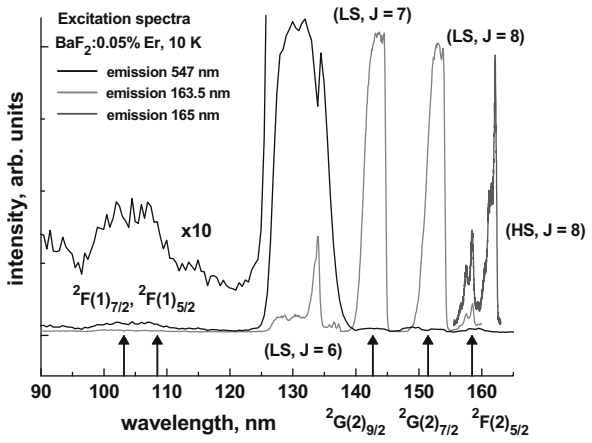

Fig. 2. Time integrated excitation spectra of Er^{3+} emissions in BaF_2:0.05 mol%Er at 10 K. The spectra have been corrected using a salicylate standard. Resolution was 0.32 nm. Black line, emission wavelength at 547 nm, step 0.5 nm, red and blue lines emission wavelengths set at 163.5 and 165 nm, step was set at 0.5 and 0.01 nm, respectively. Black arrows indicate positions of the relevant $4f^{11}$ levels. For details, see text. (For interpretation of the references to colour in this figure legend, the reader is referred to the web version of this article.)

exciton which can transfer its energy to any of the lower lying $4f^{11}$ levels (like $^4S_{3/2}$) but large relaxation prevents energy transfer to the higher lying levels of both $4f^{11}$ and $4f^{10}5d$ configurations [9].

It is interesting to note a peak and a corresponding indentation at 133.9 nm in the red and black line spectra shown in Fig. 2. This observation strongly suggests that there are two separate processes providing excitation of VUV and VIS Er emissions that compete for the excitation photons. We identify these two processes as a direct Er^{3+} d-excitation leading mostly to d–f VUV emission and an Er-bound exciton exciting f–f VIS emission of Er^{3+} [9].

None of the spectra shown in Fig. 2 reveals a significant VUV sensitivity suggesting a lack of good response to ionizing radiation. A very weak VUV signal at 547 nm is, as revealed by the emission spectrum under VUV excitation (not shown), mostly due to the STE emission and not to emission from Er ions.

The 163.5 nm emission band, dominating the spectrum shown in Fig. 3, is generated by the slow, spin forbidden optical transition between the lowest energy, high spin (HS) d-level of the $4f^{10}5d$ Er^{3+} configuration [10] and the ground state of the $4f^{11}$ Er^{3+} configuration, $^4I_{15/2}$. The corresponding band in the excitation (absorption) spectrum peaks at about 162.1 nm (blue line in Fig. 2). The two much stronger bands at 153 and 143.2 nm and the third competition-distorted band at about 133.9 nm produce the same VUV and UV emissions and are due to the spin allowed transitions from the ground $4f^{11}$ state, $^4I_{15/2}$, to higher energy states of the $4f^{10}5d$ configuration [9]. Although there is some similarity between bands at 133.9 and 162.1 nm which led us previously to a different assignment of the 133.9 nm band [9] we note that this band is strongly distorted by a competition which makes any comparisons very difficult. Also, the energy difference between the 133.9 and 153 nm bands is much lower than the 15200 cm^{-1} 10Dq lower bound value estimated from the Ce-excitation spectrum (Fig. 1).

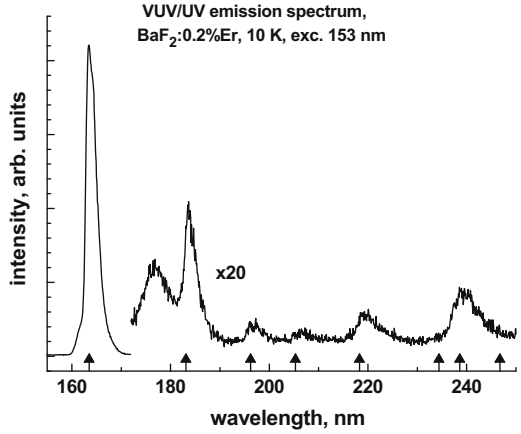

Fig. 3. Uncorrected time integrated VUV/UV emission spectrum of BaF_2:0.05 mol%Er at 10 K. Excitation was 153 nm (maximum of LS band). Resolution was 1.1 nm, step 0.1 nm. To expose fine details part of the spectrum was multiplied by a factor of 20. Arrows indicate calculated positions of d-bands corresponding to transitions from the lowest HS d-level and terminating at consecutive lowest states of the $4f^{11}$ configuration.

Despite that Ce and Er ions most likely occupy the same site and should experience the same crystal field, the number and relative positions of the high lying energy levels involving d-electrons, represented by bands in Figs. 1 and 2, are very different. Clearly the crystal field splittings of the fivefold degenerate d-level that fully explain the excitation spectrum of Ce, in no way match the structure observed for the spin-allowed bands in Er.

The origin of this structure has been proposed by van Pieterson et al. [11] to come from the excitation of the $4f^{10}$ core left behind by an electron moved to the lowest energy 5d orbital. The transition energies are therefore increased by energies corresponding to transitions between the consecutive states ($^5I_8$, $^5I_7$, $^5I_6$) of the $4f^{10}$ configuration (Ho^{3+} ion), producing higher lying bands in the excitation spectrum of the Er^{3+} d–f emission.

The bands shown in Fig. 2 have been labeled by the *J*-values corresponding to the consecutive $4f^{10}$ states reached by a given transition. The lowest states of the Er^{3+} $4f^{10}5d$ configuration must have a total spin S equal to 5/2 or 3/2 hence we have used the "LS" label to designate a spin 3/2 level and a spin-allowed transition band (the ground state is $^4I_{15/2}$, spin 3/2) while "HS" designates a spin 5/2 level and a spin-forbidden transition band.

The arrows in Fig. 2 indicate energies of $4f^{11}$ levels calculated by Piatkowski [12] in the framework of the free ion approximation by diagonalization of the appropriate energy matrix. M.F. Reid's f-shell empirical programs were used to evaluate the energy parameters. The experimental values of only low energy levels (up to 35,000 cm^{-1}) from the absorption spectrum of BaF_2:0.2 mol%Er were included in the calculations which provided, nevertheless, theoretical energies for all the states of the $4f^{11}$ configuration. The root mean square deviation between the experimental and calculated energies was 90 cm^{-1}.

Of the five states, $^2F(1)_{7/2}$, $^2F(1)_{5/2}$, $^2G(2)_{9/2}$, $^2G(2)_{7/2}$ and $^2F(2)_{5/2}$, only one, $^2F(2)_{5/2}$, fits some sharp line features in the spectra. None of the remaining four states is expected to play any role. In particular the $^2G(2)_J$ levels overlap the centers of strong allowed d-bands and any contribution from them is highly unlikely. Even if there is some weak absorption into one of those levels, it must be immediately depleted nonradiatively into the overlapping d-level as the configuration coordinate parabola of the d-level intersects the f-level parabola near its minimum.

In Fig. 3 we show time-integrated emission spectrum under 153 nm excitation (d-band) at 10 K. The spectrum has not been corrected for spectral sensitivity of the set-up. To aid presentation two different vertical scales have been used to expose fine details of the spectrum. The arrows indicate calculated positions of bands corresponding to transitions originating at the lowest d-level and terminating at the lowest levels of the $4f^{11}$ configuration. The agreement between experimental and calculated positions of bands in the VUV range of wavelengths is reasonably good.

In Fig. 4 we present a time-integrated excitation spectrum of the $^4S_{3/2}$–$^4I_{15/2}$ green Er emission at 10 K for the sample of (Ba,La)F_2:0.2 mol% of Er. The spectrum resembles the spectrum measured for VUV emissions in Er-activated BaF_2 and shown in Fig. 2

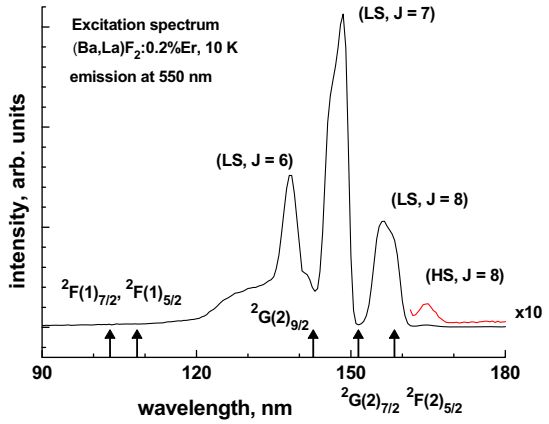

Fig. 4. Time integrated excitation spectrum of Er emission at 550 nm in $(Ba,La)F_2$:0.2 mol%Er at 10 K. Resolution was 0.32 nm, step 0.5 nm. The red line shows part of the spectrum multiplied by 10 to expose the low intensity HS band peaking at 165 nm. Arrows indicate calculated positions of $4f^{11}$ levels. (For interpretation of the references to colour in this figure legend, the reader is referred to the web version of this article.)

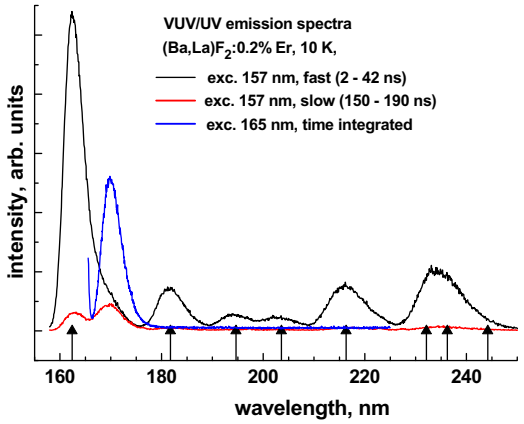

Fig. 5. Uncorrected VUV/UV emission spectra of $(Ba,La)F_2$:0.2 mol%Er at 10 K. Black and red lines present time resolved emission spectra under 157 nm (LS band) excitation. Resolution was 1.1 nm, step 0.1 nm. Blue line presents time integrated emission spectrum under 165 nm excitation (HS band). Resolution was 1.1 nm, step 0.05 nm. Arrows indicate calculated positions of d-bands corresponding to transitions originating from the lowest LS level and should be compared to positions of the spin-allowed "fast" bands (black line). (For interpretation of the references to colour in this figure legend, the reader is referred to the web version of this article.)

(red and blue lines). The red trace shows the same spectrum in the range of the spin-forbidden transition to the lowest (HS, $J = 8$) $4f^{10}5d$ state multiplied by a factor of 10 in order to expose a weak spin-forbidden band on the short wavelength side of the first spin-allowed band peaking at 157 nm. We note that positions of all the bands in $(Ba,La)F_2$ are shifted in comparison to BaF_2; the (HS, $J = 8$) band peaks at 164.6 instead of 162.1 nm, the (LS, $J = 8$) band peaks at 157 instead of 153 nm, the (LS, $J = 7$) band peaks at 148.5 instead of 143.2 nm and the (LS, $J = 6$) band peaks at 138.1 instead of 133.9 nm. The shift of d-bands reflects the change in crystal field brought about by a large La co-doping; the resultant massive presence of compensating fluorine interstitial ions is expected to change (increase) the low symmetry crystal field component. The low symmetry crystal field component is responsible, together with the spin-orbit coupling, for splitting of the 5d(e) levels. For larger splittings we expect a lower transition energy, hence a red shift of relevant absorption bands, as observed experimentally.

We note that shifts of d-levels results in the change of relative positions of $4f^{11}$ levels. Calculated positions of the five relevant $4f^{11}$ levels are shown by arrows. We observe that the two $^2G(2)_J$ levels no longer overlap the maxima of LS bands but fall between them and the $^2F(2)_{5/2}$ level, which, in BaF_2, was positioned half way between the LS and HS bands, now overlaps the LS band.

In Fig. 5 we show the time resolved VUV/UV emission spectra of $(Ba,La)F_2$:Er under excitation into the 157 nm, spin-allowed band where the black line presents "fast", and a red line - "slow" time window spectra. There is also shown a time-integrated emission spectrum under excitation into the 165 nm spin-forbidden band. The "slow" spectrum clearly demonstrates that most of the emission is fast (the decay time is 46 ns) but there is also a slowly decaying band at 170 nm at the longer wavelengths side of the dominant "fast" band at 162.3 nm that becomes visible for longer delays. The "slow" band at 170 nm dominates the spectrum under the 165 nm excitation corresponding to the spin-forbidden transition to the lowest HS state of the $4f^{10}5d$ configuration, as expected.

We observe that in both materials, BaF_2:Er and $(Ba,La)F_2$:Er, the VUV emission resulting from direct excitation into the lowest energy (HS, $J = 8$) level, is slow, as expected. This is no longer the case for higher d-level excitations. In BaF_2:Er excitation into the 153 nm LS band is followed by relaxation and slow emission from the (HS, $J = 8$) level. In $(Ba,La)F_2$:Er excitation into the LS band at 157 nm band corresponding to the (LS, $J = 8$) level, is followed by a fast, spin-allowed emission from the same level with almost no relaxation to the lower (HS, $J = 8$) level.

The obvious conclusion must be that relaxation between the lowest LS and HS levels is strongly enhanced when the $^2F(2)_{5/2}$ level is positioned between them. This is the case in BaF_2 but in $(Ba,La)F_2$, where stronger lower symmetry crystal field component shifts the lowest d-levels downwards, is not.

In Fig. 6 we show a simple configuration coordinate model for the three relevant electronic states of the Er^{3+} ion in BaF_2 and $(Ba,La)F_2$, $4f^{11}$ $^2F(2)_{5/2}$, $4f^{10}5d$ (HS, $J = 8$) and $4f^{10}5d$ (LS, $J = 8$). We assume that all the $4f^{11}$ states, in particular the ground state $^4I1_{5/2}$ (not shown) and the $^2F(2)_{5/2}$ state (black solid line) assume equilibrium positions for the same value of the configuration coordinate, namely zero. The equilibrium positions of the two lowest energy $4f^{10}5d$ state parabolas were chosen to fit experimental values of appropriate transitions from absorption (excitation) and emission spectra. From the figure it is clear that in BaF_2 the $^2F(2)_{5/2}$ parabola

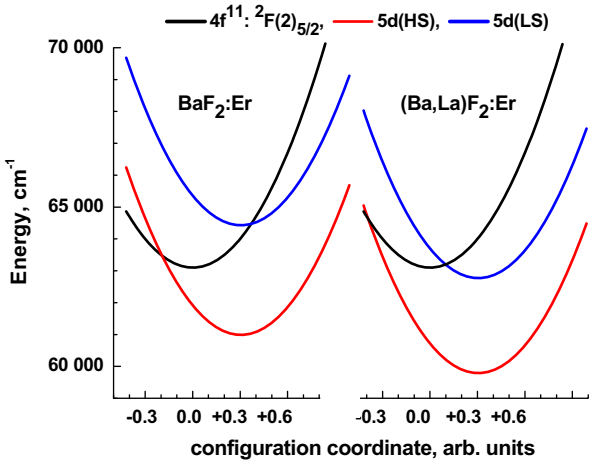

Fig. 6. Configuration coordinate diagrams showing energies of two $4f^{10}5d$ states, (HS, $J = 8$) and (LS, $J = 8$), and one $4f^{11}$ state, $^2F(2)_{5/2}$ of Er^{3+} ion in BaF_2 (left), and $(Ba,La)F_2$ (right). The parabolas of the excited $4f^{11}$ state and the ground $4f^{11}$ state, $^4I_{15/2}$, assume minimum energy at zero. The equilibrium positions of d-states parabolas have been shifted to fit experimental transition energies from excitation and emission spectra. Note the shifts of d-level electronic energies responsible for relative position of the $4f^{11}$ level. (For interpretation of the references to colour in this figure legend, the reader is referred to the web version of this article.)

intersects the two $4f^{10}5d$ parabolas in such a way that it may contribute to the nonradiative transition (relaxation) between them. In (Ba,La)F_2 situation is different and nonradiative relaxation between the two d-levels must be, and apparently is, much slower.

4. Summary and conclusion

In this paper we have presented selected examples illustrating the significance of VUV spectroscopy in studies of wide bandgap materials activated with rare earth ions.

VUV/UV excitation spectra help to identify and evaluate various channels of energy transfer from the host to the emitting ion. We have pointed out that, in addition to direct excitation of the ion, there is also a fast and efficient channel involving excitons bound to the ion. Direct optical excitation into the band corresponding to this process is followed by fast and efficient emission with no delay and no rise time. On the contrary, free excitons are unlikely to transfer their energy to the ions creating, instead, self-trapped excitons (STE).

We note that for the rare earth bound exciton a significant fraction of energy is lost to lattice relaxation so that, consequently, no VUV/UV emission can be excited and observed.

The VUV excitation with photon energies exceeding bandgap energy generates free electron-hole pairs that may be consecutively trapped and recombined in the vicinity of the rare earth ion with transfer of recombination energy to the ion. Since the intermediate step in this process involves the rare earth bound exciton no high energy $4f^{n-1}5d$ or $4f^n$ levels can be excited. Consequently the Ce^{3+} ion with its near UV d–f transition stands a chance to be good radiative recombination center while Er^{3+}, emitting in the VUV/UV, does not.

The VUV excitation spectra provide, therefore, a convenient test revealing how good a given material is in response to ionizing radiation. This is important in applications involving detection of gamma and/or X-ray radiation.

We have demonstrated that comparison between excitation spectra of light (here Ce) and heavy (Er) rare earth ions reveals interesting and important differences in their electronic structure.

The excitation spectra of heavy ions reveal additional weak bands corresponding to spin-forbidden transitions from the ground state to the exchange split HS states of the $4f^{n-1}5d$ configuration. Unlike for the Ce^{3+} ion, for which the structure of excited states is fully described by the crystal field split d-level, in Er^{3+} the excited states of the $4f^{10}5d$ configuration are determined by excited states of the d-electron as well as of the $4f^{10}$ configuration, changing the number and positions of bands in the excitation (absorption) spectrum.

We have also demonstrated that studies of VUV emission and excitation spectra can provide important information concerning radiative and nonradiative relaxation of highly excited rare earth ions. In particular we have demonstrated that nonradiative relaxation between consecutive LS and HS energy levels of the Er^{3+} $4f^{10}5d$ configuration may be relatively slow. In consequence it is possible to observe fast and efficient emission from the LS level as in Er activated (Ba,La)F_2. In BaF_2:Er, where d-levels are shifted because of modified crystal field, fast nonradiative relaxation from the LS to HS level is facilitated by a $4f^{11}\ ^2F(2)_{5/2}$ level located almost exactly halfway between them. Consequently the VUV emission of BaF_2 is dominated by slow, spin-forbidden transition between the HS level of the $4f^{10}5d$ configuration and the ground state $4f^{11}\ 4I_{15/2}$.

Acknowledgments

The crystals used in this study have been offered by late Prof. Alex Lempicki of Boston University who supported me and the group from N. Copernicus University for many years. I also gratefully acknowledge Prof. Georg Zimmerer and Dr Gregory Stryganyuk from Hasylab for help and hospitality during Superlumi experiments, Prof. M.F. Reid of Canterbury University, Christchurch, New Zealand for his f-shell empirical programs to calculate lanthanide ions $4f^{11}$ energy levels. I am grateful to Dawid Piatkowski who actually performed these calculations and to Sebastian Janus, Robert Theis and Kinga Jastak, who took part in experiments at Hasylab. I also thank DESY and EC for financial support during Superlumi experiments under Contract RII3-CT-2004-506008 (IA-SFS).

References

[1] R.T. Wegh, A. Meijerink, R.J. Lamminmäki, J. Hölsa, J. Lumin. 87–89 (2000) 1002–1004.
[2] P.S. Peijzel, A. Meijerink, R.T. Wegh, M.F. Reid, G.W. Burdick, J. Solid State Chem. 178 (2005) 448.
[3] R.T. Wegh, E.V.D. van Loef, G.W. Burdick, A. Meijerink, Mol. Phys. 101 (2003) 1047.
[4] G. Zimmerer, Nucl. Instrum. Methods Phys. Res. A 308 (1991) 178.
[5] A.J. Wojtowicz et al., Hasylab Annual Report 1998, Hamburg 1998: <http://hasyweb.desy.de/science/annual_reports/1998/part1/contrib/22/521.pdf>.
[6] W.J. Manthey, Phys. Rev. B8 (1973) 4086.
[7] G.J. Hollingsworth, D.S. McClure, Phys. Rev. B48 (1993) 13280.
[8] J.W. Hodby, in: W. Hayes (Ed.), Crystals with the Fluorite Structure, Clarendon Press, Oxford, 1974, p. 24.
[9] A.J. Wojtowicz, Opt. Mater. 31 (2009) 474–478.
[10] (a) R.T. Wegh, H. Doker, A. Meijerink, Phys. Rev. B57 (1998) R2025; (b) R.T. Wegh, A. Meijerink, Phys. Rev. B60 (1999) 10820.
[11] (a) L. van Pieterson, M.F. Reid, A. Meijerink, Phys. Rev. Lett. 88 (2002) 067405; (b) L. van Pieterson, M.F. Reid, G.W. Burdick, A. Meijerink, Phys. Rev. B65 (2002) 045114.
[12] A.J. Wojtowicz, S. Janus, D. Piatkowski, presented at ICL 08, Lyon, submitted to J. Lumin.